ISSN 0915-633X

NATIONAL INSTITUTE FOR FUSION SCIENCE

Physics and Engineering Design Studies on Large Helical Device

O. Motojima, K. Akaishi, K. Fujii, S. Fujiwaka, S. Imagawa, H. Ji, H. Kaneko, S. Kitagawa, Y. Kubota, K. Matsuoka, T. Mito, S. Morimoto, A Nishimura, K. Nishimura, N. Noda, I. Ohtake, N. Ohyabu, S. Okamura, A. Sagara, M. Sakamoto, S. Satoh, T. Satow, K. Takahata, H. Tamura, S. Tanahashi, T. Tsuzuki, S. Yamada, H. Yamada, K. Yamazaki, N. Yanagi, H. Yonezu, J. Yamamoto, M. Fujiwara, and A. Iiyoshi

(Received – Jun. 22, 1992)

NIFS-161 Aug. 1992

RESEARCH REPORT
NIFS Series

NAGOYA, JAPAN

PHYSICS AND ENGINEERING DESIGN STUDIES ON LARGE HELICAL DEVICE

O.Motojima, K.Akaishi, K.Fujii, S.Fujiwaka, S.Imagawa, H.Ji, H.Kaneko, S.Kitagawa, Y.Kubota, K.Matsuoka, T.Mito, S.Morimoto, A.Nishimura, K.Nishimura, N.Noda, I.Ohtake, N.Ohyabu, S.Okamura, A.Sagara, M.Sakamoto, S.Satoh, T.Satow, K.Takahata, H.Tamura, S.Tanahashi, T.Tsuzuki, S.Yamada, H.Yamada, K.Yamazaki, N.Yanagi, H.Yonezu, J.Yamamoto, M.Fujiwara, and A.Iiyoshi

National Institute for Fusion Science, Nagoya 464-01

ABSTRACT

The construction of the Large Helical Device (LHD) is progressing as a 7 year project in Japan which began in 1990. This year, necessary research and development programs are nearly reaching the final goal of the original schedule and we have started the construction of the basic parts of LHD. We report on the results of the physics and engineering design studies, and the recent status of the construction of LHD.

Keywords: Large Helical Device, currentless system, steady-state, superconductor, divertor, heliotron, helical field, nuclear fusion

1. Introduction

The Large Helical Device (LHD) is a toroidal magnetic fusion experimental apparatus which will contribute to the physics understanding of currentless, steady-state and non-axisymmetric toroidal plasmas with high temperature and high beta values being extrapolatable to the reactor regime [1],[2],[3]. This project also aims to contribute to the development of several fusion technology areas, primarily superconductivity, mechanics and materials research. LHD has the prospect of providing an alternative and complementary method to the general fusion approach by tokamak devices.

The superconducting (SC) coil system is composed of $\ell=2$ helical coils and three sets of poloidal coils with a total stored magnetic energy of 1.63 GJ. The main machine parameters, m number, ℓ number, major radius, coil minor radius, magnetic field, plasma minor radius, and plasma volume are 10, 2, 3.9 m, 0.975 m, 4 T, 0.65 m, and 30 m^3, respectively. The specifications are listed in Table 1. These basic parameters were decided based on the detailed physics analyses and optimization studies on the transport, MHD, high energy particle orbit containment, divertor effect, etc. trying to maximize the surpassing properties of LHD [4]. A view of the experimental rooms and the cross-section of LHD are shown in Fig. 1. The most remarkable difference from tokamak plasmas is the availability of currentless steady-state operation, which explores new physics issues, especially gaining the freedom from the current profile constraint and the probability of the current disruptions. It is eventually a final goal of LHD project to demonstrate these issues. From the engineering view point, the property of the steady-state operation and the absence of the plasma current and the disruption contribute to reduce the requirements or the constraints on the technological specifications. These are the primary factors which have directed the LHD construction to be a superconducting machine.

Three sets of heating systems, gyrotrons, NBI, and ICRF will be constructed. The total amount of the power absorbed is expected to be more than 20 MW. The currentless plasma will be initiated by microwave power (84 GHz, 10 MW). According to the neoclassical heating scenario, an electron root condition obtained by the specific electron heating is expected to increase the ion temperature subsequently with the combination of large NBI heating power (125 kV, 15 MW) [5],[6]. The highest ion temperature expected

is around 10 keV. The longest confinement is obtained by increasing the density and getting an ion root condition. These investigations of the confinement properties and heating efficiency are very important in establishing the reactor ignition scenario by helical systems. As for the experiment to produce a steady-state plasma, a maximum power level of 3 MW is injected into the vacuum vessel.

High beta experiments are another highlight of the program. The expected maximum volume averaged beta value is 5 %, which is the necessary value for future fusion reactors. This is the result of new physics findings which conclude that it is possible to maintain the magnetic well which is effective for obtaining a stable high beta plasma even in the case that the magnetic axis was shifted inside the torus where the orbit loss of high energy ions is remarkably reduced [7]. The expected plasma parameters are listed in Table 2 and the objective parameter range is shown in Fig. 2, which is the Lawson diagram with the present tokamak data-base.

The material of the superconductor is NbTi, and the cooling systems are pool-boiling for the helical coils and forced-flow for the poloidal coils. Conductors with large currents up to 30 kA have been newly developed using an aluminum stabilizer in addition to the copper matrix. LHD has a divertor to control the steady-state particle recycling and to improve the confinement by almost twice (H-mode production). The vacuum vessel has a dumbbell-shaped poloidal cross-section making it possible to install a closed divertor chamber. We have recognized the importance of the studies on the boundary plasma, i.e., effects of magnetic shear, density gradient and electric field, etc. These considerations have been taken into account in the design criteria to increase the flexibility of LHD as an experimental device for physics research.

The construction schedule is shown in Table 3. In 1991, we have started the construction of the inner vertical field coil, the helical coil fabrication machine, and the cryostat. The latter two will be completed in 1993. The main experimental building will also be completed at the end of 1993. Immediately after the completions of the building and facilities, we will be able to begin manufacturing the helical coils in the Toki site in 1994. It takes one year and a half. The vacuum vessel will then be assembled which takes about one year. Therefore LHD will be completed in 1997.

In the following sections, we summarize the results of physics and engineering design studies of the Large Helical Device which occupies an important role for fusion research. We then report on the present status of progressing R&D, engineering design and construction of LHD.

2. Objectives of LHD and the Results of Physics Design Studies

Recent fusion experiments by large tokamak devices have shown remarkable progress which provided the achievement getting close to the break even condition of Q=1 [8]. In the Joint European Tokamak (JET) device, tritium was first brought into deuterium plasmas and this experiment attracted a lot of attention in the world [9]. In such a setting of fusion research, LHD approach is considered to increase in importance, since it is a major alternative approach to provide the currentless steady-state plasmas [1].

The major missions of LHD are; (1) to study transport for a wide range of plasma parameters ($T(0) \lesssim 10$ keV, and $n\tau T = 2 \sim 10 \times 10^{19}$ keV·s/m^3), (2) to produce a high beta value of 5 %, and (3) to attain quasi-steady-state operation using a helical divertor [10]. These parameters are thought to constitute a least necessary minimum to extrapolate the experimental data base obtained by LHD to the reacting plasma regime in order to develop future plasma physics studies [11][12]. The objective area is already shown in Fig. 2. We will use hydrogen or deuterium gas and neutral beams. The experimental schedule has been carefully chosen to be complementary to the tokamak approaches. We now have to recognize the long term perspective of fusion research. In the end of this decade, fusion research will be directed to go through the construction of a demonstration reactor after compiling enough data sets from the on-going experiments. To exploit a new approach and to supply the complementary data base for the existing tokamaks, LHD should be completed within several years. Therefore, the completion of LHD is scheduled for 1997. This timing coincides with the completion of the ITER EDA phase [13].

LHD has a magnetic configuration with medium rotational transform, shear and well. LHD utilizes continuous helical windings which is called the heliotron/torsatron type. In Japan, we have developed this type of field configuration over many years which is called heliotron series [14]. Namely,

we have the typical originality and historical background of this research. This is one of the major reasons why National Institute for Fusion Science (NIFS) was established and the LHD project was born in 1989 in Japan. As is well known, there is a wide variety of helical field configurations. Looking around the world-wide research activities on helical systems, it is necessary to describe the modular stellarator approach pursued by Germany with Wendelstein VII-AS [15]. As is shown in Fig. 2, after the proof of principal experiment on the helical system producing the temperature of 1,000 eV, plans for the next step were proposed by Japan and Germany. The former is LHD and the latter is Wendelstein VII-X (W VII-X) [16]. Since W VII-X utilizes a modular coil system, the magnetic field configuration is extremely different from that of LHD. These two devices are complementary to each other. Moreover the independent approaches are viable to develop the present research of helical systems extending further toward the fusion condition.

Design efforts have been concentrated on the optimization of machine parameters self-consistently satisfying the physics requirements and engineering constraints [17]. It was necessary for the LHD engineering design to bring out good physics properties of confinement and MHD, and long confinement capability for high energy particles. The magnetic surfaces should have the following features: enough distance between the wall and plasma boundary, good mod-B structure (shape of the constant-magnetic-field structure), enough magnetic shear θ (up to$\sim$0.4), magnetic wells (up to 1.5%) and large connection length of the magnetic field lines for typical divertor field lines ($L \sim 3 \cdot 2\pi R$). There are three major criteria for the LHD designing tasks, i.e.,

(1) loss rate of the high energy particle (η_{loss}) is small enough to attain the heating efficiency (η_h) greater than 70 %,

(2) $\beta \geq 5$ %,

and

(3) $w_{dw} \geq 3$ cm (distance between plasma boundary and first wall).

The results of pitch number (m) optimization is shown in Fig. 3. There are three limiting lines i.e., stability and equilibrium β, and divertor criteria, which correspond to the above criteria of (2) and (3). To satisfy the criteria (1) and (2), we found that the shift of the plasma axis inwards by about

15 cm works preferably. In this case, the stability β value is improved a lot, since LHD is a fat and low aspect ratio helical device. Here, the requirement for the low aspect ratio is inevitable for advanced commercial reactors. This property makes it possible to install a large tangential injection port for NBI. In the case of tangential NBI, it was made clear that the heating efficiency is much better than 70 % [3]. The value of 70 % is a criterion for the perpendicular heating method, i.e., ICRF.

As shown in Fig. 1, there are three pairs of poloidal coils. These poloidal coils produce primarily the dipole field and quadrupole field [12]. Their positions are optimized to minimize the stray field from LHD. The former is used for the shift of the magnetic axis which is effective to change the MHD properties and the confinement of the high energy particle orbit. The shift of the axis varies the plasma performance widely. The dynamic range of the shift is ± 30 cm at a magnetic field strength of 4 T. The typical results are shown in Fig. 4 as a summarized form which was obtained by Todoroki and his co-workers [18]. Shifting the axis inwards, the beta value of 5 % is obtained and the loss rate of the high energy particles is reduced to be less than 10 %. The latter is used to control the ellipticity which is thought effective to improve the neoclassical transport and to reduce the bootstrap current. Since the LHD project aims to produce currentless plasmas, we are sensitive to control the bootstrap current. Nakajima and Okamoto [19] predicted that the vertical elongation carries out the reduction of the bootstrap current. When an excess amount of the bootstrap current is excited, in the extreme case, we have to adopt the inverse current drive technique. Our design criterion for the bootstrap current is 300 kA supposing a 10 ms disruption which is equivalent to 150 kA and a 1 ms disruption. These criteria primarily come out from preventing the destruction of the vacuum vessel due to the magnetic forces by eddy current induced by the disruption. Another important role of the poloidal coils is the real time control of the coil current, because LHD is an experimental device. The maximum design value of the field changing rate is less than 0.5 T/s at 6 T which is much smaller than in tokamak devices. The real time control of the poloidal coil current requires further engineering solutions and an increase of the construction costs. However, this scenario is thought necessary to expand the dynamic range of the LHD experiment.

One more important technique to increase the feasibility of the physics experiment is the current profile control of the helical coil. This is attained dividing the helical coil package into three sub-coils, which is shown in Fig. 5 (H1-I, M, and O). This is a new idea proposed for the LHD [1]. Varying the current ratio of three layers of the helical coil, we can widely change the basic magnetic parameters. Especially it is important that γ_c is varied from 1.1 to 1.4. The available range is shown in Fig. 3 with a box. The extended range of γ_c is wide enough to cover the various magnetic parameters which bring experimentalists a wide flexibility. For example, we can vary the boundary ι value from 0.8 to 1.5. This is almost equivalent to install toroidal coils in LHD like in the Heliotron E device in Kyoto University [14].

3. Engineering Design of LHD

From the engineering viewpoint, much attention has been paid to the following areas;(1) superconducting helical coils, (2) superconducting poloidal coils, (3) vacuum vessel with divertor, (4) power supply and coil protection circuit, (5) control system, and (6) refrigeration system. In this section, the engineering aspects of LHD are described.

The outer diameter of LHD is ~13 m and the total weight is ~1,500 t, whereof helium cooled weight is 910 t (helical coils: 140 t, poloidal coils: 120 t, support structure: 600 t and other components: 50 t). Helical coils, poloidal coils and supporting structure are combined together and cooled down to the helium temperature in the toroidal cryostat. The necessary cooling-down time is about two weeks. There is an extra-vacuum boundary inside the cryostat, i.e. the plasma vacuum vessel which has a shape like a dumbbell and is installed between helical coils and the plasma. Since the total amount of the hoop and vertical magnetic force exceeds 350 kt and 240 kt, respectively, which corresponds to the peak value of 1,000~1,500 t/m, the design effort to develop the solid structural support configuration is very important. A major part of the support is composed of the coil vessel, shell arm, shell and rib structure. These are shown in Fig. 6. Consistent design was required to compromise the different conditions or criterions, i.e., deformation during coil cooling-down phase and magnetic field

excitation, accuracy for manufacturing and setting, rigidity of coil package, mutual movement of conductor, etc. The major part of the magnetic force is supported by the LHe cooled shell. The material is SUS with low permeability (less than 1.02). The advantage of LHD as a steady-state machine was exploited extremely. One typical result is that it is not necessary to install any toroidal electric break in the support and the vacuum vessel. This certainly made the engineering design more feasible compared to SC tokamak devices.

3.1 Helical Coil

The helical coil is designed using pool boiling type conductors with enough aluminum and copper as stabilizers to realize a high current density. The requirement on the current density from the physics side was very strict. Increasing the current density, the harmonics of the current distribution become more preferable. It becomes possible to get a clear boundary and enough distance between plasma and coil surface if we are able to select the harmonics appropriately. Eventually, the target value for the package current density is 53.3 A/mm^2 at 9.2 T.

During the evaluation of selecting the superconducting material and the cooling system, we decided to use the abundant experience to manufacture superconducting coils with NbTi. Historically, it helped this decision that the initial physics concept definition study decided the maximum field strength at the plasma center to be 4 T corresponding to the value of about 9 T on the coil surface. It was also necessary to avoid degradation of the critical current (I_c) due to the strain effect during the helical coil fabrication. Therefore, the material Nb_3Sn could not be the candidate.

Required accuracy is ± 2 mm for the helical coils. The deformation due to the magnetic force should be suppressed to less than ± 3.5 mm in the case of 4 T operation. Since the dangerous components of the error field are the lower harmonics of toroidal (n) and poloidal (m) directions, joint, turn over and feed through sections are carefully designed and distributed calculating the effect of the error field caused by the deviation of coil current from the original place. The welding procedure of the coil vessel, arm support and shell support is the critical path to attain the above criterion.

The magnetic field strength will be increased by two steps. The magnetic field at the conductor is initially 6.9 T (central field 3 T, phase I) and then increased to 9.2 T (4 T, phase II). Therefore, the temperature of the coil is planned to be decreased from 4.4 K to 1.8 K in the phase II experiment using superfluid He II. The coil is fully stabilized during the phase I experiment satisfying Maddock's criterion, and will be dynamically stabilized during the phase II experiment enhancing the heat transition rate through the coil surface by means of Helium II. The smooth transition of LHD program from phase I to phase II experiments will establish a new engineering consequence for superconductivity. We have newly started the R & D programs for developing the scenario of the He II cooling. The most difficult engineering issue recognized in this transition is the feasibility of imposing a further temperature gradient between the 4.2 K shell support and the 1.8 K helical coil in a limited space. The extra thermal shield cooled by LHe will be necessarily installed between the helical coil vessel and LN_2 shield which is shown in Fig. 5.

3.2 Poloidal Coil

The poloidal coil is cooled by forced flow of supercritical helium. The type of conductor is the so-called cable-in-conduit one. Inlet and outlet temperatures of the coolant are 4.5 K and 4.8 K, respectively. The current of the three sets of poloidal coils (IV, IS, and OV) are 5.0 MA, -4.5 MA, and -4.5 MA, respectively. Though the poloidal coils compose an additional coil system against the helical coils, the magnetic force on the poloidal coil is comparable to the helical coil. This means that scrupulous R & D was also necessary for poloidal coil construction. Their shape is simpler than that of the helical coil. However, the diameter of the biggest OV coil is large enough to require new technological development. This may be understood from the fact that the total stored energy of the poloidal coil set reaches 0.7 GJ. Since the peak magnetic force level also reaches 1,000 t/m, we have initially developed an idea of the sliding support to attach the poloidal coils to the shell support. The major reason was that the poloidal coil has more mechanical rigidity than the helical coil. Since the estimated equivalent Young's moduli of the coil package are 8,000 kg/mm^2 and 2,000 kg/mm^2 in hoop and vertical directions, respectively, it was considered

possible that the hoop stress could be supported by the poloidal coils themselves. However, the estimated heat produced by friction was so large (10 kW in total, friction constant 0.3) that we abandoned this direction. They will be attached directly to the shell support increasing its stiffness.

3.3 Conductor Development

The most urgent subject to be solved in a superconducting coil design is the development of a viable superconductor which carries a large current of around 30 kA [1]. From the point of view of large magnetic force (1,000～1,500 t/m) and torsional angle (Max～50°/m), a NbTi conductor was selected. We are developing several candidates of the conductor, in which aluminum is used to satisfy the improved stability criterion. In Fig. 7(a), the cross-sections of two major candidates of the conductor are shown. The location and amount of aluminum and distribution of NbTi strands are different in each design. First of all, it was necessary to study the uniformity of the current distribution in the conductor. We have investigated this point developing several kinds of conductors with different strand distributions, i.e. uniform distribution type, multi-layer distribution type, and transposed structure type [20]. The critical current of the conductors has been successfully confirmed, and no difference was found on the conductor capability due to the difference of the location of the aluminum stabilizer. Anisotropic current distribution has not been observed.

To evaluate the performance of conductors and to make the final selection, I_c, the recovery current, etc. has been investigated in detail concentrating our efforts on the two conductors shown in Fig. 7(a). In Fig. 7(b), one of the results is shown [20]. The specification of the conductor is shown in Table 4. The recent results suggested that the combination of aluminum and copper requires an understanding of the microstructure of the current path, i.e. the current redistribution appears when the quench occurs. The stiffness of the conductor is also an important subject. It was investigated with a 500 t mechanical stress test machine. Since the stress level of the insulation between layers or turns of conductors exceeds 15 kg/mm^2, the selection of the material requires a careful design effort. The coverage ratio of the insulator to the conductor surface should be more than 50%. The candidate of the material of the stiff insulator is GFRP with

three dimensional glass cloth which is newly developed. We have a plan to spend at least one year in selecting the insulating material carrying out the careful evaluation tests from now.

Feasibility research of the coil fabrication is investigated from several kinds of the practical R & D small model coils (R~1 m, B~2 T, m=3~4). They are listed in Table 5. The necessary data base for the coil fabrication has been already obtained and now, the test coils are just before the cooling down test.

3.4 Support Configuration

Here, we present the results of the stress analysis. The deformation and the stress/strain of helical coils and support structures have been analyzed with a finite element method (FEM) code. The critical issue for designing the support structure is to develop a reasonable structural design which ascertains the necessary and high accuracy of the helical coils, because the stress level and the degree of the deformation strongly depend on the idea of the structural design. In Fig. 8, the typical results of the deformation with the FEM code (ANSYS) are presented for the structural shell, where the averaged thicknesses of the helical coil vessel and structural shell are 50 mm and 100 mm, respectively. Spatial restrictions by ports are taken into account in the calculation. From this figure, we can find the deformation of each mesh point from the original position. Although we chose a typical example to show the tendency of the deformation simply in this figure, the rib support was not taken into account in the calculation. Therefore, the maximum deformation of the helical coils reaches about 6 mm. However, we finally reduced the deformation of the shell support to ± 3.5 mm by increasing the rigidity by the rib support. This calculation confirmed the consistent supporting design. The maximum stress appears on the inside surface of the helical coil vessel and reaches 35 kg/mm^2. The maximum stress level of the shell support is also about 35 kg/mm^2. These values are acceptable for the structural material stainless steel.

3.5 Vacuum Vessel

The complicated three dimensional shape of the vacuum vessel is required to supply sufficient room for the closed divertor system. Since LHD is an

experimental device for plasma physics research, more than 40 ports are installed on the vacuum vessel. The shape of the vacuum vessel is understandable with Fig. 1(b) and Fig. 6. The distance between the surface of the plasma and port flanges is only 1.5 m which may be less than the radial thickness of the toroidal coils of big tokamak devices and provides a lot of accessibility to the experimentalists. The biggest one with a lozenge shape is located on the outer equatorial plane. The size is 1.2 m x 1.1 m. The total amount of the port area reaches $\sim$20 m^2, which accounts to $\sim$10 % of the total vessel surface. The baking temperature of the vacuum vessel is about 100 ℃, and that of the divertor carbon tiles is 350 ℃. The expected heat flux on the divertor plate is 1 kW/cm^2 for a 5 s discharge with 30 MW of heating power input. This value is comparable to the output of the tokamak engineering reactor design. The cooling water pipes of the vacuum vessel are fabricated on the inner surface (plasma side) allowing the necessary maintenance.

We have developed an R & D model for the vacuum vessel of LHD. It is a full size model to explore the fabrication technique of the vacuum vessel. The vacuum vessel will be fabricated after completing the helical coils. Therefore the procedure to construct the vacuum vessel is specially planned and developed.

As shown in Fig. 3, one of the critical issues of the vacuum vessel design is that the gap between the helical coil and plasma is limited, especially on the inboard side of the torus. The available distance between the helical coil and first wall including the coil vessel must be less than 15 cm to leave enough distance between the first wall and the plasma and to avoid severe plasma-wall interaction. This is shown in Fig. 5. It means that an accurate fabrication and assembly of the vessel ($\sim\pm$5 mm) are required.

We have considered two types of mechanical loading on the vessel, which are atmospheric and magnetic ones. The latter is produced when the poloidal fields are changed with time or the bootstrap current disappears in a short time period. The FEM was also adopted to evaluate the stress level and deformation of the vacuum vessel. The most severe stress due to the atmospheric force appears near the largest port in the equatorial plane. It is close to the value of 15 kg/mm^2. The magnetic loading appears when a large eddy current is induced by a sudden disruption of the induced plasma

current. In our LHD design, we suppose a finite probability of the current disruption when some residual current exists. One typical case is the disruption triggered by the drop of a graphite tile from the top of the vacuum vessel. The design criterion is based on the condition to withstand the magnetic loading due to 150 kA/1 ms (or 300 kA/10 ms) current disruption. In the high $n\tau T$ plasma production, in which the bootstrap current becomes maximum and its flow in the direction increases the vacuum rotational transform angle, the direction of the magnetic force is outward which is the same as that of the atmospheric force. It is concluded from the FEM analysis that the thickness of 15 mm is sufficient for the vacuum vessel to satisfy the design criterion. This value is close to the limiting thickness for reliable fabrication of the vacuum vessel after the completion of the helical coil fabrication.

4. Summary

The LHD project is now progressing on schedule. The necessary R & D programs are reaching the final goal of the original schedule and producing the necessary and useful data base which contributes to the development of fusion technology. During both the physics and engineering design and R & D, we have already developed new ideas and subsequent results which are the major issues of this paper. Here in Fig. 9, we try to summarize the possible areas covering both plasma physics and fusion technology, where the major contributions of the LHD project primarily appear. The LHD project is contributing to plasma physics knowledge and fusion technology development which are indispensable in accelerating world-wide fusion research.

REFERENCES

[1] MOTOJIMA, O., et al., Plasma Physics and Controlled Nuclear Fusion Research, Washington, 3 (1990) 513

[2] IIYOSHI, A., et al., Fusion Technology 17 (1990) 169

[3] DESIGN GROUP Report, Green Book (1987) March, Blue Book (1988) March Orange Book (1989) March

[4] NIFS LHD Technical Report 1 (1990)

[5] NAKAMURA, Y., et al., PPLK Report 24 (1988), PPL, Kyoto University

[6] TAKEIRI, Y., et al., Proceedings of the 16th Symposium on Fusion Technology, London, (1990) 1012

[7] SANUKI, H., et al., NIFS Report 9 (1989)

[8] The JET Team, 13th International Conference on Plasma Physics and Controlled Nuclear Fusion Research, Washington, IAEA-CN-53/A-3-4 (1990)

[9] Private communication with the JET Team

[10]OHYABU, N., et al., To be published in Proceedings of International Conference on Plasma Surface Interaction, Monterey, Ca, 1992 March 30-April 3

[11]MOTOJIMA, O., IEEE Transactions of Magnetics 27 (1991) 2214

[12]YAMAZAKI, K., et al., Plasma Physics and Controlled Nuclear Fusion 2 (1990) 709

[13]ITER Concept Definition, ITER-1, 1988

[14]UO, K., et al., Plasma Physics and Controlled Nuclear Fusion Research 2 (1987) 355

[15]RENNER, H., et al., 13th International Conference on Plasma Physics and Controlled Nuclear Fusion Research, Washington, IAEA-CN-53/C-1-2 (1990)

[16]GRIEGER, G., et al., 13th International Conference on Plasma Physics and Controlled Nuclear Fusion Research, Washington, IAEA-CN-53/G-1-6 (1990)

[17]MOTOJIMA, O., et al., Fusion Technology 1988, eds. A.M.Van Ingen (Elsevier Science Publishers B.V., Amsterdam, 1988), pp.402

[18]TODOROKI, J., et al., Plasma Physics and Controlled Nuclear Fusion Research, 2 (1988) 637

[19]NAKAJIMA, N., and OKAMOTO, M., J.Phys. Society Japan 59 (1990) 3595

[20]MITO, T., et al., In Proceedings of 12th International Conference on Magnet Technology, Leningrad, USSR, June 23-28, 1991, MT-12 AL-5

FIGURE CAPTIONS

Fig. 1 (a) A bird's-eye view of the main experimental building
(b) The poloidal cross-section and the side view of LHD

Fig. 2 Objective parameter range of LHD and data points obtained

Fig. 3 Results of physics optimization
γ_c: Coil pitch parameter, m: Pitch number of the helical coil
A_p: Coil aspect ratio R_c/a_c
There are three important criteria: equilibrium, stability β, and divertor clearance Δ_{dw}.

Fig. 4 Parameter dependence versus the axis shift
a_p: Plasma minor radius , β : Plasma beta value, ι (0): Magnetic rotational transform angle of the field line on the axis,

η_s: Loss rate of the high energy particles

Fig. 5 Cross-section of the helical coil package

Fig. 6 Structure of the support and the vacuum vessel

Fig. 7 (a) Cross-sections of the newly developed conductors
(b) Result of conductor R & D on the critical current

Fig. 8 Deformation of the shell support by the FEM calculation

Fig. 9 Summary of the possible contribution of LHD on plasma physics and fusion technology

Table 1 SPECIFICATIONS

	PHASE I	PHASE II
MAJOR RADIUS	3.9 ■	←
COIL MINOR RADIUS	0.975 ■	←
AVERAGED PLASMA RADIUS	0.5～0.65 ■	←
PLASMA ASPECT RATIO	6～7	←
ℓ	2	←
■	10	←
γ ○=■/2·$a_{○}$/R (PITCH PARAM.)	1.25	←
α (PITCH MODULATION FACTOR)	0.1	←
MAGNETIC FIELD		
CENTER	3 T	4 T
COIL SURFACE	6.9 T	9.2 T
HELICAL COIL CURRENT	5.85 MA	7.8 MA
COIL CURRENT DENSITY	40 A/■■^{2}	53 A/■■^{2}
NUMBER OF LAYERS	3	←
LHe TEMPERATURE	4.4 K	1.8 K
POLOIDAL COIL CURRENT	STEADY	REAL TIME
INNER VERTICAL COIL	5.0 MA	←
INNER SHAPING COIL	-4.5 MA	←
OUTER VERTICAL COIL	-4.5 MA	←
LHe TEMPERATURE	4.5 K	4.5 K
PLASMA VOLUME	20～30 ■^{3}	←
ROTATIONAL TRANSFORM		
CENTER	<0.5	←
BOUNDARY	～1	←
HELICAL RIPPLE AT SURFACE	0.2	←
PLASMA DURATION	10 s	←
REPETITION TIME	5 ■in	←
HEATING POWER		
ECRH	10 MW	←
NBI	15 MW	20 MW
ICRF	3 MW	9 MW
STEADY	-----	3 MW
$D^{\circ} \rightarrow D^{+}$	-----	PRACTICE
NEUTRON YIELD	-----	$2.4X10^{17}$ n/shot
COIL ENERGY	0.9 GJ	1.6 GJ
REFRIGERATION POWER	5～7 kW	10～15 kW

Table 2 TARGET PLASMA PARAMETERS

HIGH n τ T MODE

$T_i = 3 \sim 4$ keV 、 $\bar{n} = 10^{14}$ cm^{-3}

$\tau_E = 0.1 \sim 0.3$ s

B = 4 T

HIGH T_i MODE

$T_i(0) = 10$ keV、 $\bar{n} = 2 \times 10^{12}$ cm^{-3}

B = 4 T

HIGH β MODE

$\beta \gtrsim 5\%$、 B = 1 ～ 2 T

Table 3 Construction Schedule of LHD

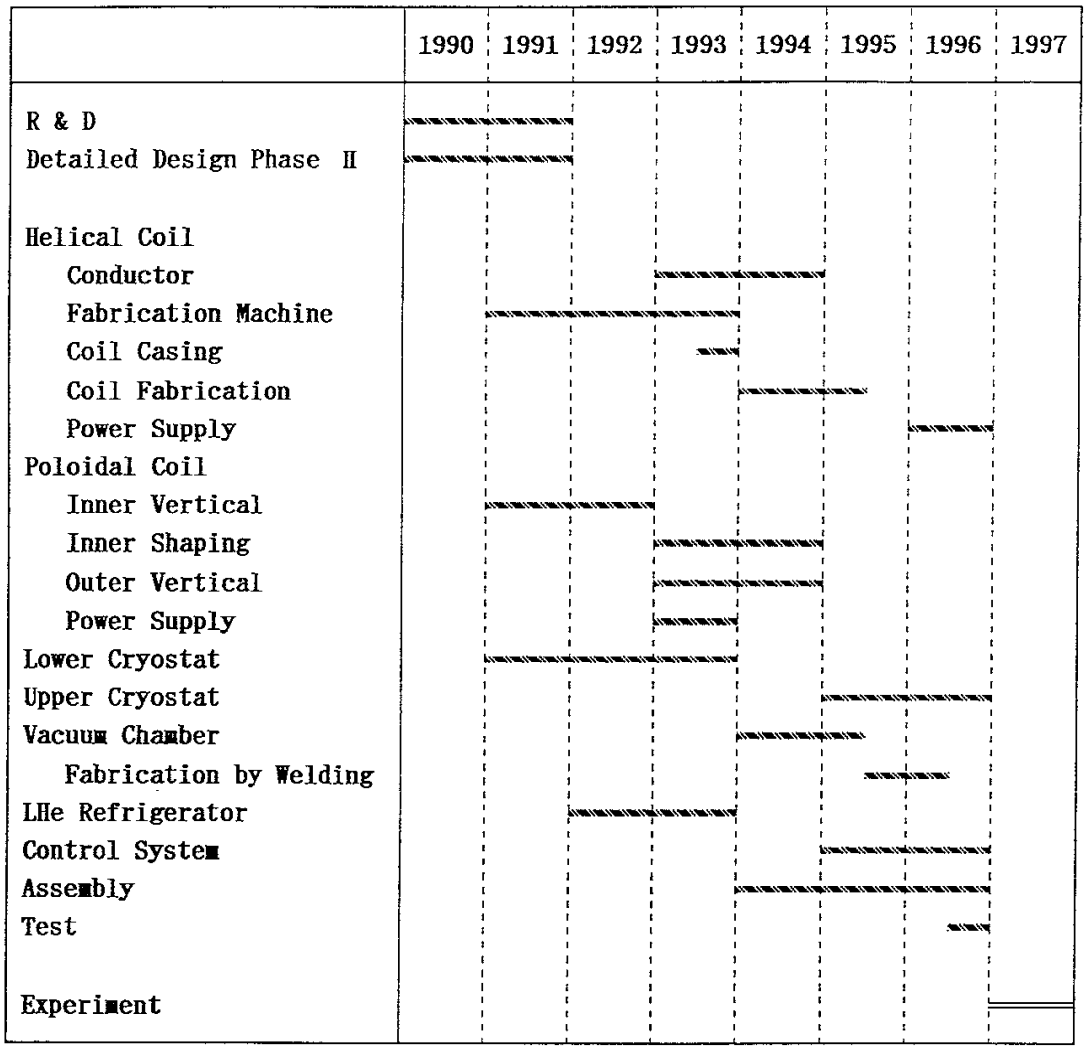

Table 4 Parameters of Conductors for LHD Helical Coils

		KISO-4B-R	Design-M
Superconductor		NbTi	←
Nominal current			
Phase I (6.9 T, 4.4 K)		21.2 kA	←
Phase II (9.2 T, 1.8 K)		28.3 kA	←
Overall current density			
Phase I (6.9 T, 4.4 K)		58.7 A/mm^2	←
Phase II (9.2 T, 1.8 K)		78.4 A/mm^2	←
Size		19.0 mm X 19.0 mm	←
Surface treatment		Copper oxide	←
Critical current (8 T*, 4.2 K)		43 kA	38 kA
Critical current density of NbTi (8 T*, 4.2 K)		1100 A/mm^2	1070 A/mm^2
Number of strands		84	58
Diameter of strand		1.05 mm	1.22 mm
Cu/SC ratio in strand		0.9	1.0
Diameter of filament		28.5 μm	25 μm
Number of filaments		726	1213
Twist pitch of filament		20 mm	17.0 mm
Twist direction of filament		inner right outer left	left for all layers
Number of cable layers		2	5
Twist pitch of cable		inner 232 mm outer 254 mm	127 mm for all layers
Twist direction		inner left outer right	right for all layers
Cross section	Total	361.0 mm^2(100%)	361.0 mm^2(100%)
	Al	83.4 mm^2 (23%)	83.0 mm^2 (23%)
	NbTi	38.9 mm^2 (10%)	36.1 mm^2 (10%)
	Cu	216.9 mm^2 (60%)	223.8 mm^2 (62%)
	PbSn	25.6 mm^2 (7%)	18.1 mm^2 (5%)

* Total field including conductor self-field

Table 5 R&D Devices

TYPE	COOLING	SPECIFICATIONS
(1) HELICAL ℓ =2, m=16	POOL- BOILING	R=0.3 m, a_c=0.063 m B=2.0 T, I=0.775 kA
(2) HELICAL ℓ =1, m=3	POOL- BOILING	R=0.8 m, a_c=0.2 m B=3.0 T, I=8.93 kA
(3) HELICAL ℓ =1, m=4	FORCED- FLOW	R=0.9 m, a_c=0.25 m B=2.77 T, I=8.08 kA
(4) TWO DOUBLE PANCAKES	FORCED- FLOW	R=0.82 m B=2.76 T, I=25 kA
(5) S-SHAPED MODULE	POOL- BOILING	R=1.4 m B=7.5 T, I=20 kA

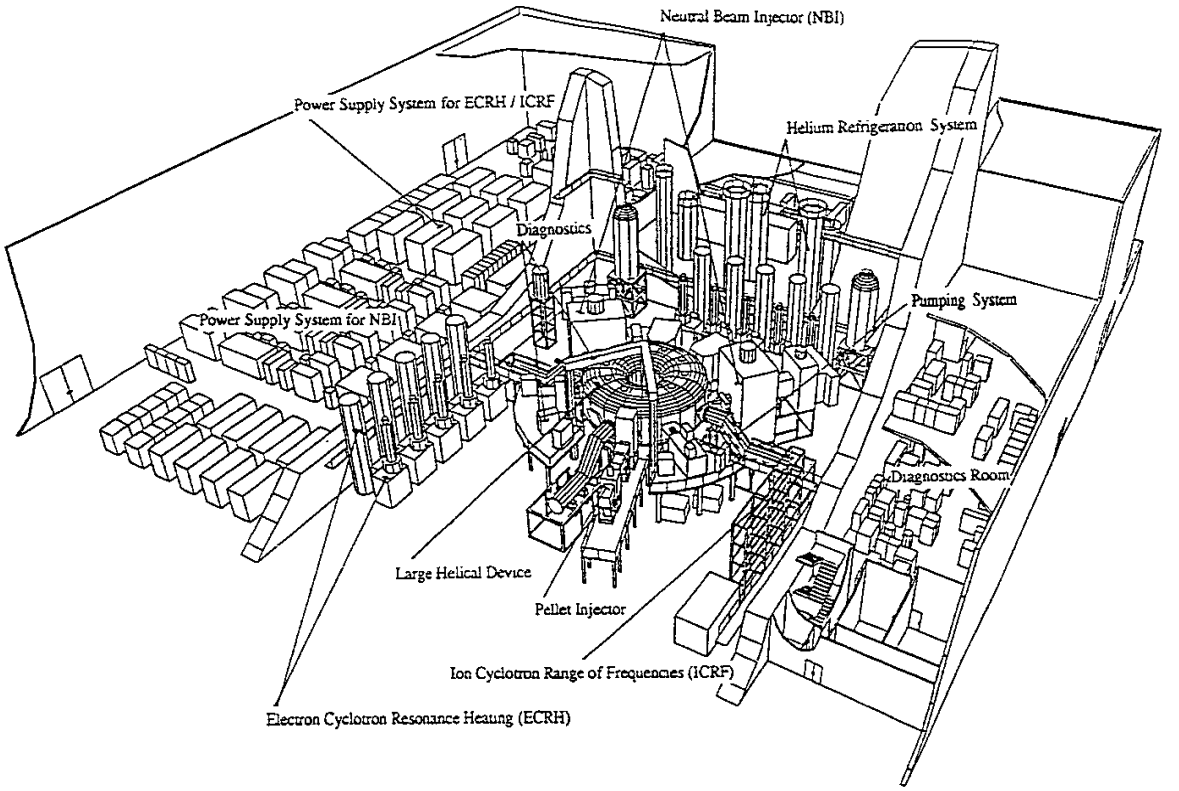
Neutral Beam Injector (NBI)
Power Supply System for ECRH / ICRF
Helium Refrigeranon System
Diagnostics
Power Supply System for NBI
Pumping System
Diagnostics Room
Large Helical Device
Pellet Injector
Ion Cyclotron Range of Frequencies (ICRF)
Electron Cyclotron Resonance Heating (ECRH)

(a)

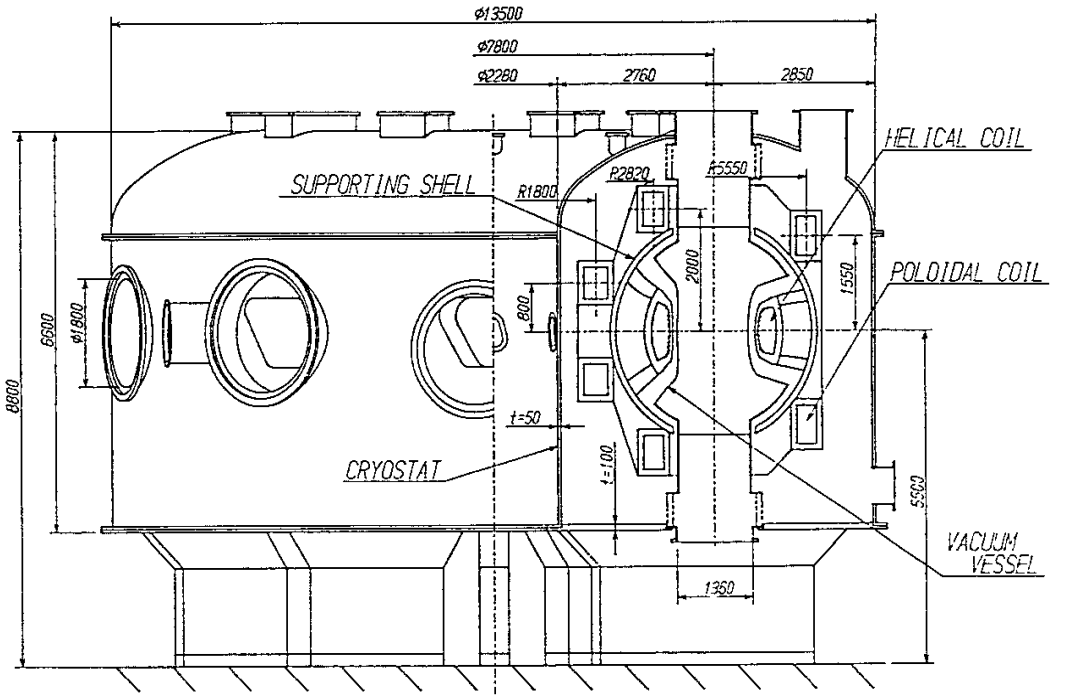
φ13500
φ7800
φ2280
2760
2850
HELICAL COIL
SUPPORTING SHELL
R1800
P2820
5550
2000
1550
POLOIDAL COIL
800
φ1800
6600
8800
t=50
CRYOSTAT
t=100
5560
VACUUM VESSEL
1360

(b)

Fig. 1

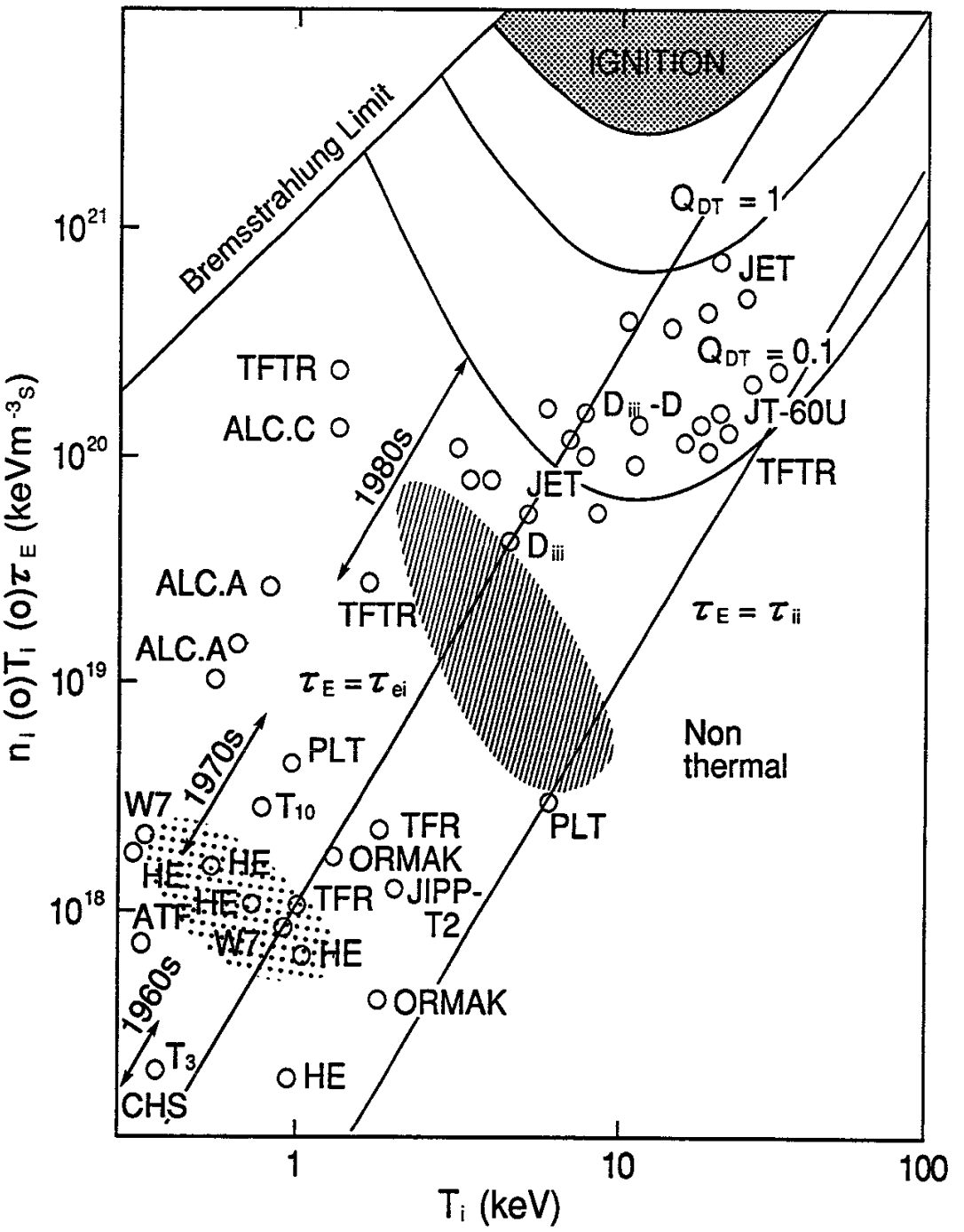
IGNITION
Bremsstrahlung Limit
Q_{DT} = 1
JET
Q_{DT} = 0.1
TFTR
ALC.C
D_{iii}-D
JT-60U
1980s
JET
TFTR
D_{iii}
ALC.A
TFTR
$\tau_E = \tau_{ii}$
ALC.A
$\tau_E = \tau_{ei}$
Non
thermal
PLT
1970s
W7
T_{10}
TFR
PLT
HE
HE
ORMAK
HE
HE
TFR
JIPP-
T2
ATF
W7
HE
1960s
ORMAK
T_3
HE
CHS
10^{21}
10^{20}
10^{19}
10^{18}
1
10
100
$n_i(o)T_i(o)\tau_E$ (keVm^{-3}s)
T_i (keV)

Fig. 2

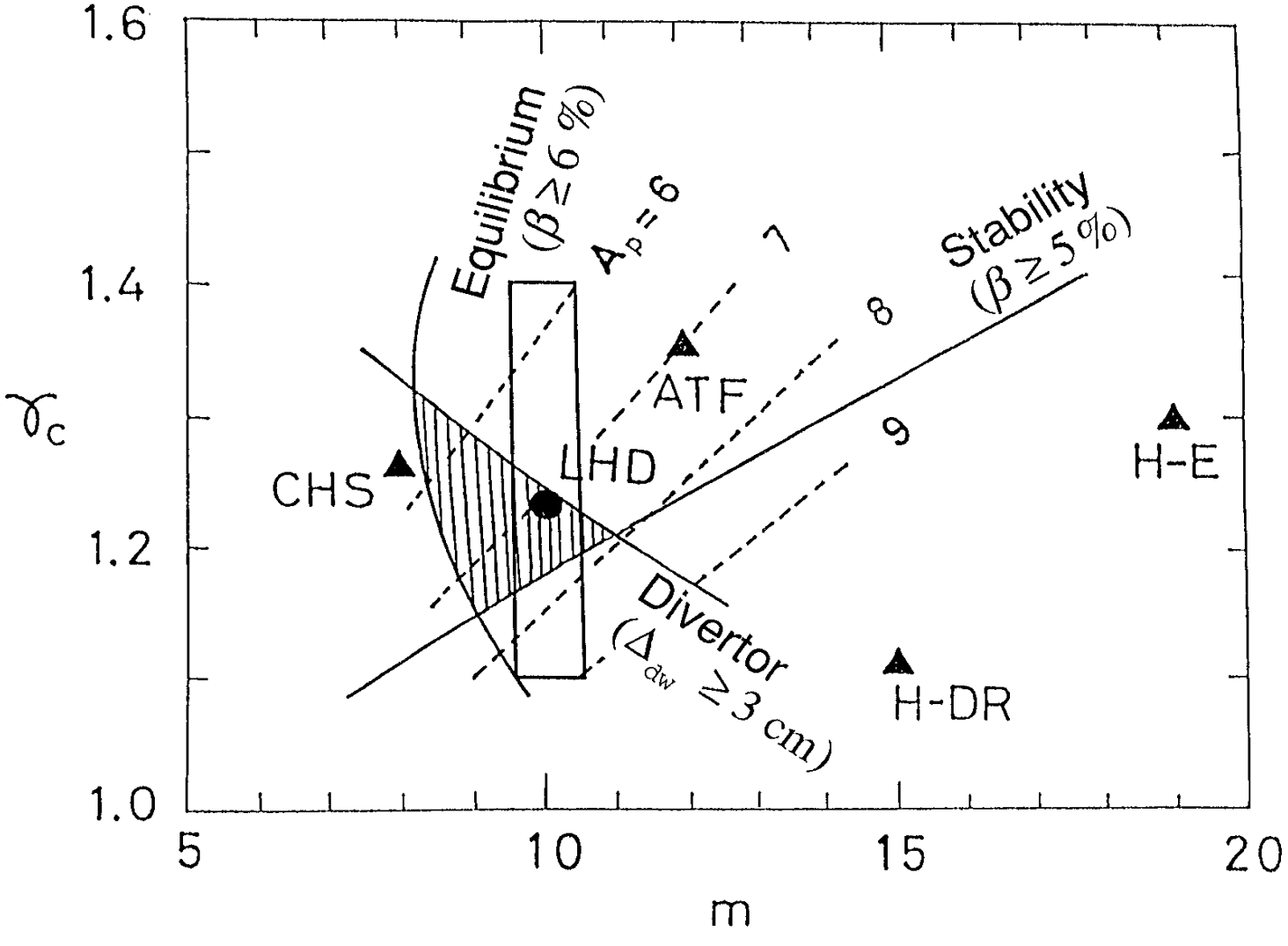
1.6
1.4
1.2
1.0
γ_c
5
10
15
20
m
Equilibrium
($\beta \geq 6\%$)
$A_p = 6$
7
8
9
Stability
($\beta \geq 5\%$)
ATF
LHD
CHS
H-E
H-DR
Divertor
($\Delta_{dw} \geq 3$ cm)

Fig. 3

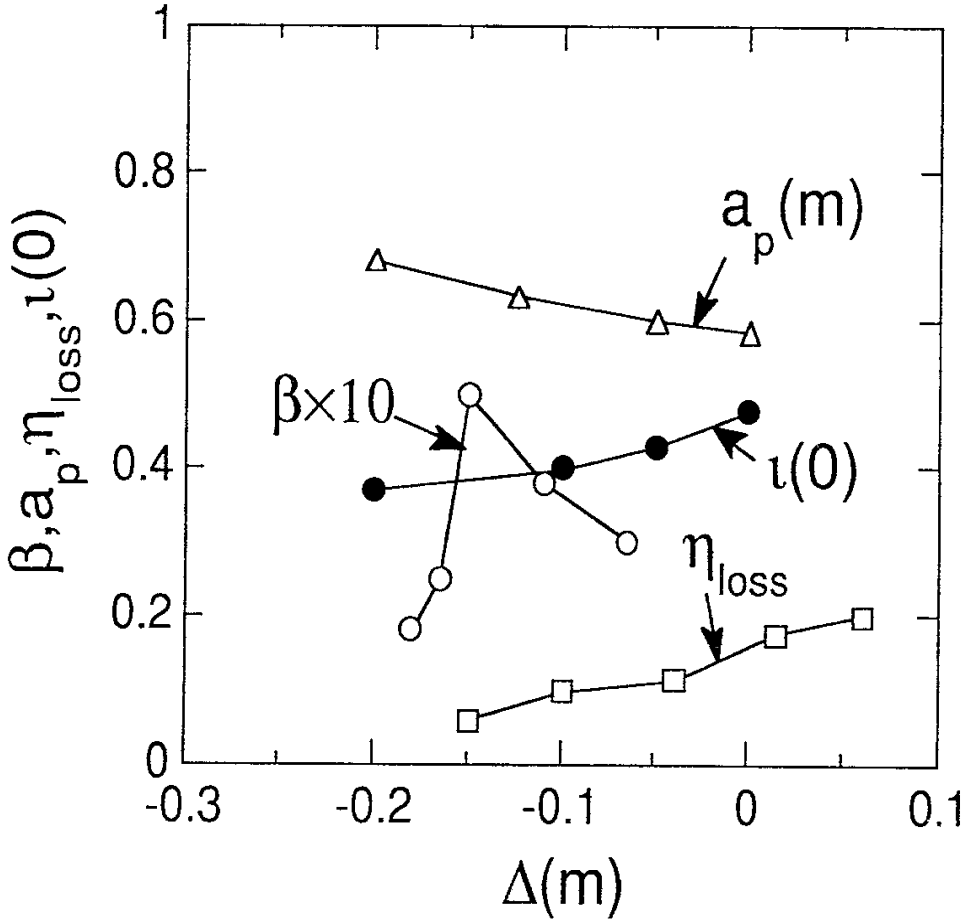

Fig. 4

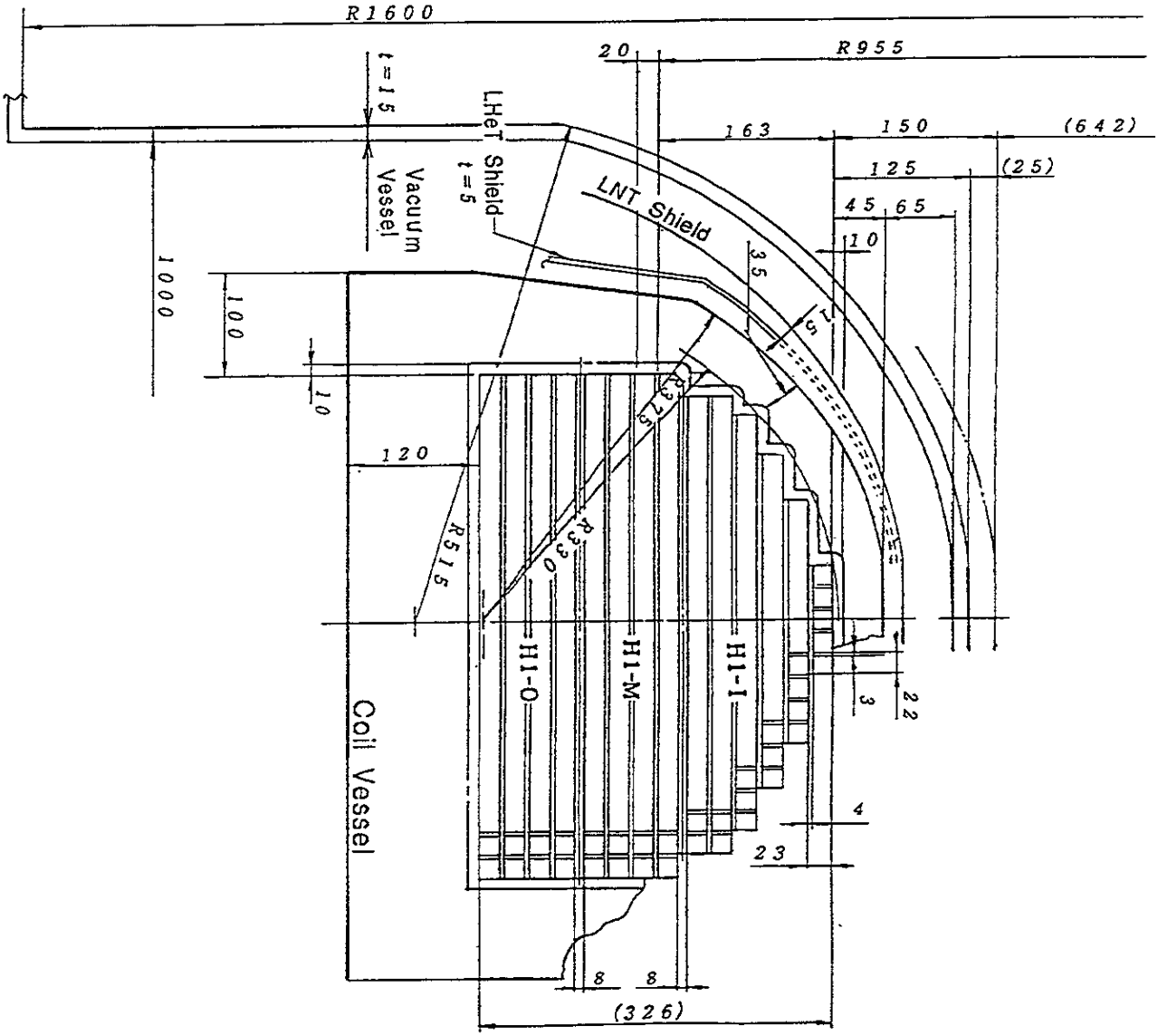
R1600
R955
20
t=15
LHeT Shield
t=5
Vacuum Vessel
LNT Shield
163
150
(642)
125
(25)
45
65
10
35
1000
100
10
120
R515
R350
H1-O
H1-M
H1-I
Coil Vessel
3
22
4
23
8
8
(326)

Fig. 5

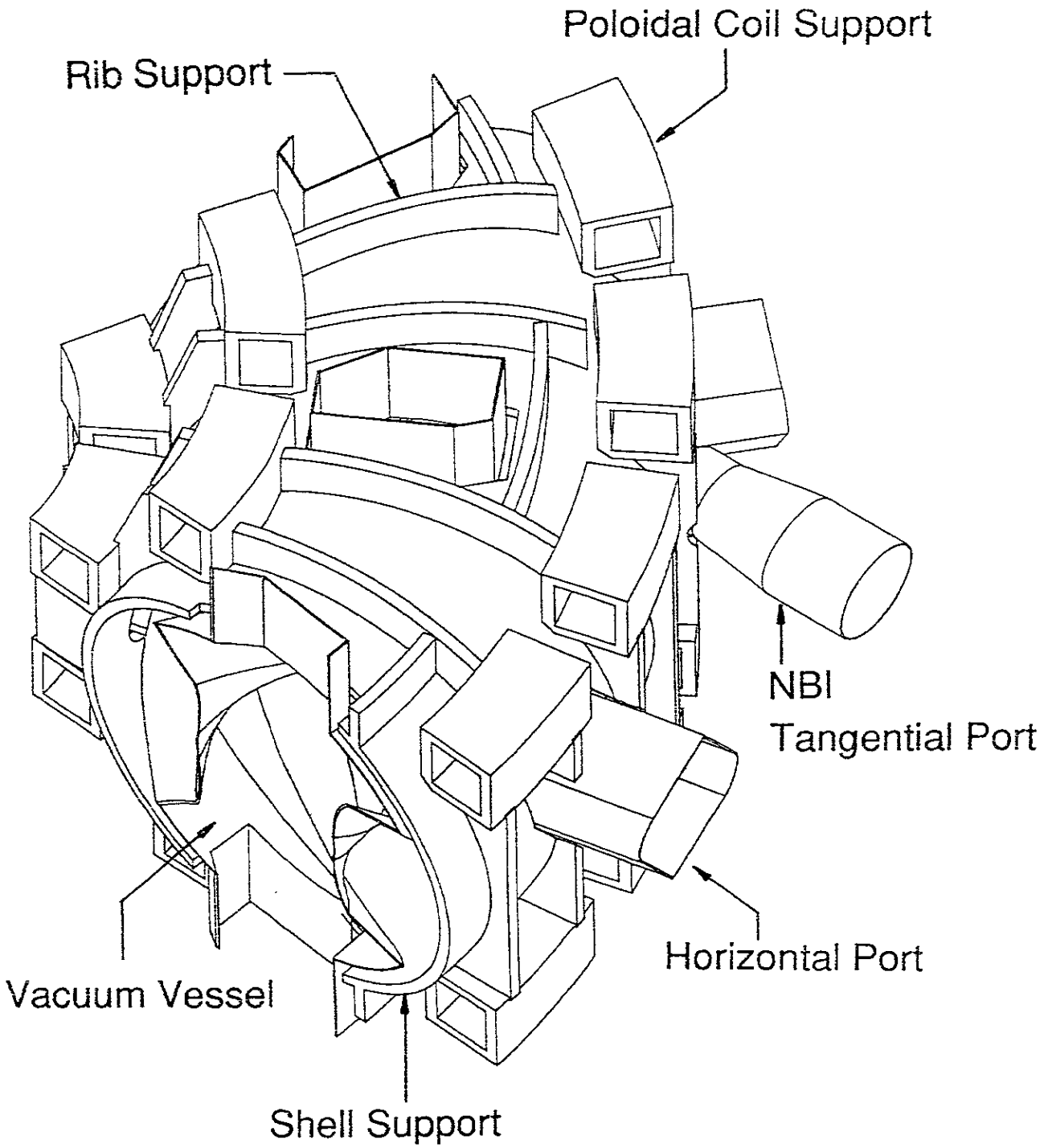
Poloidal Coil Support
Rib Support
NBI
Tangential Port
Horizontal Port
Vacuum Vessel
Shell Support

Fig. 6

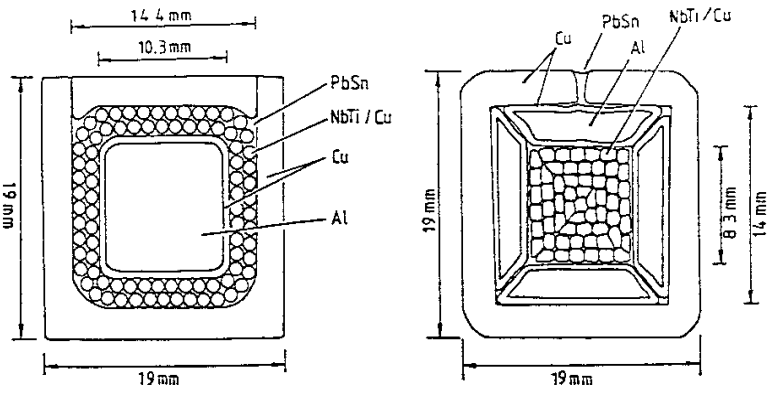

KISO-4B-R Design-M

(a)

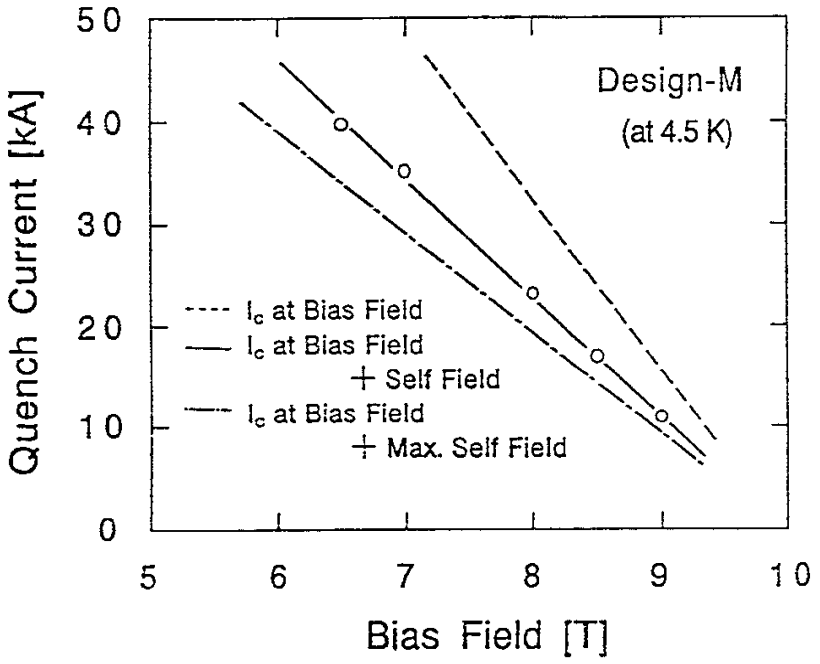

(b)

Fig. 7

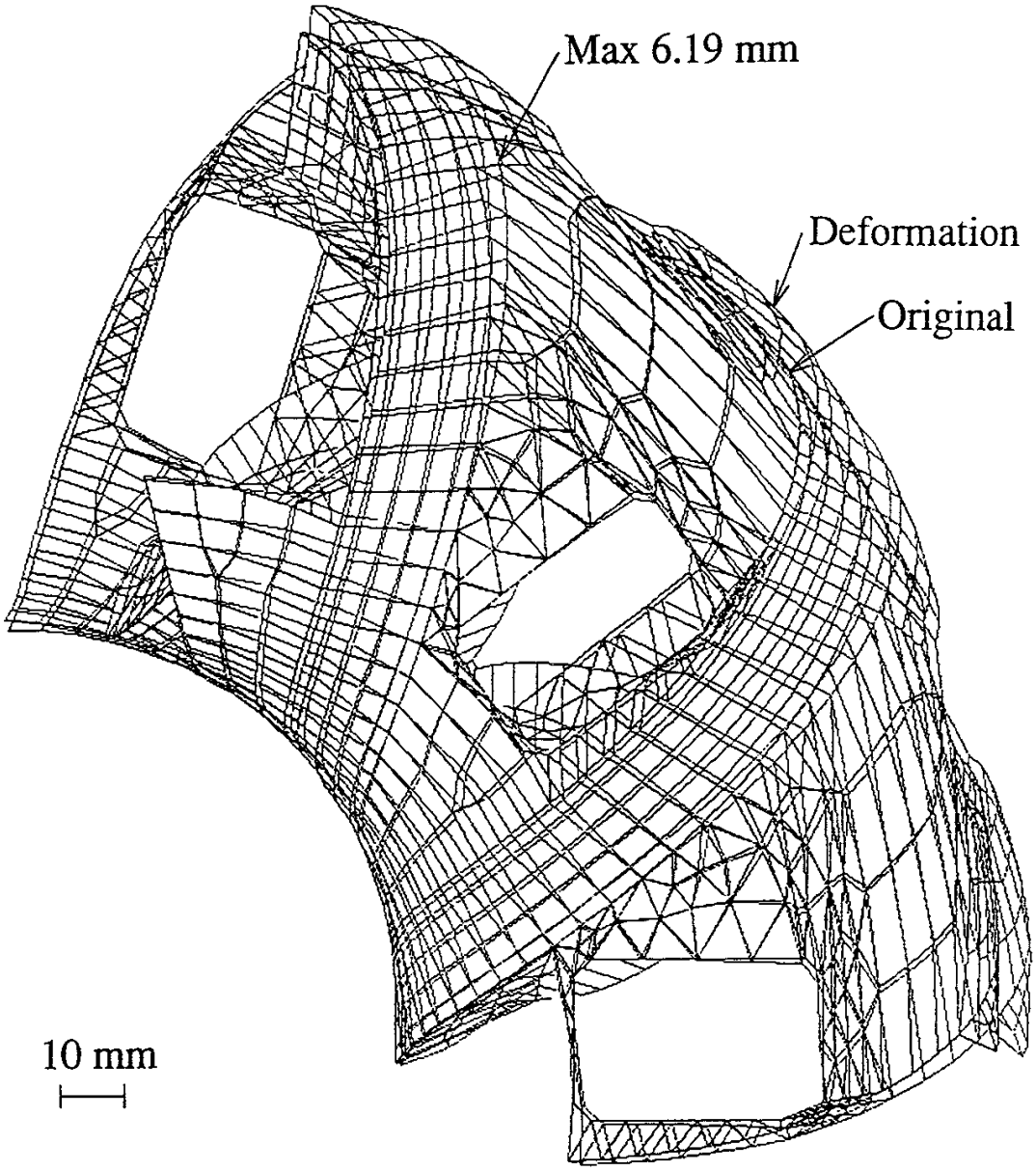

Fig. 8

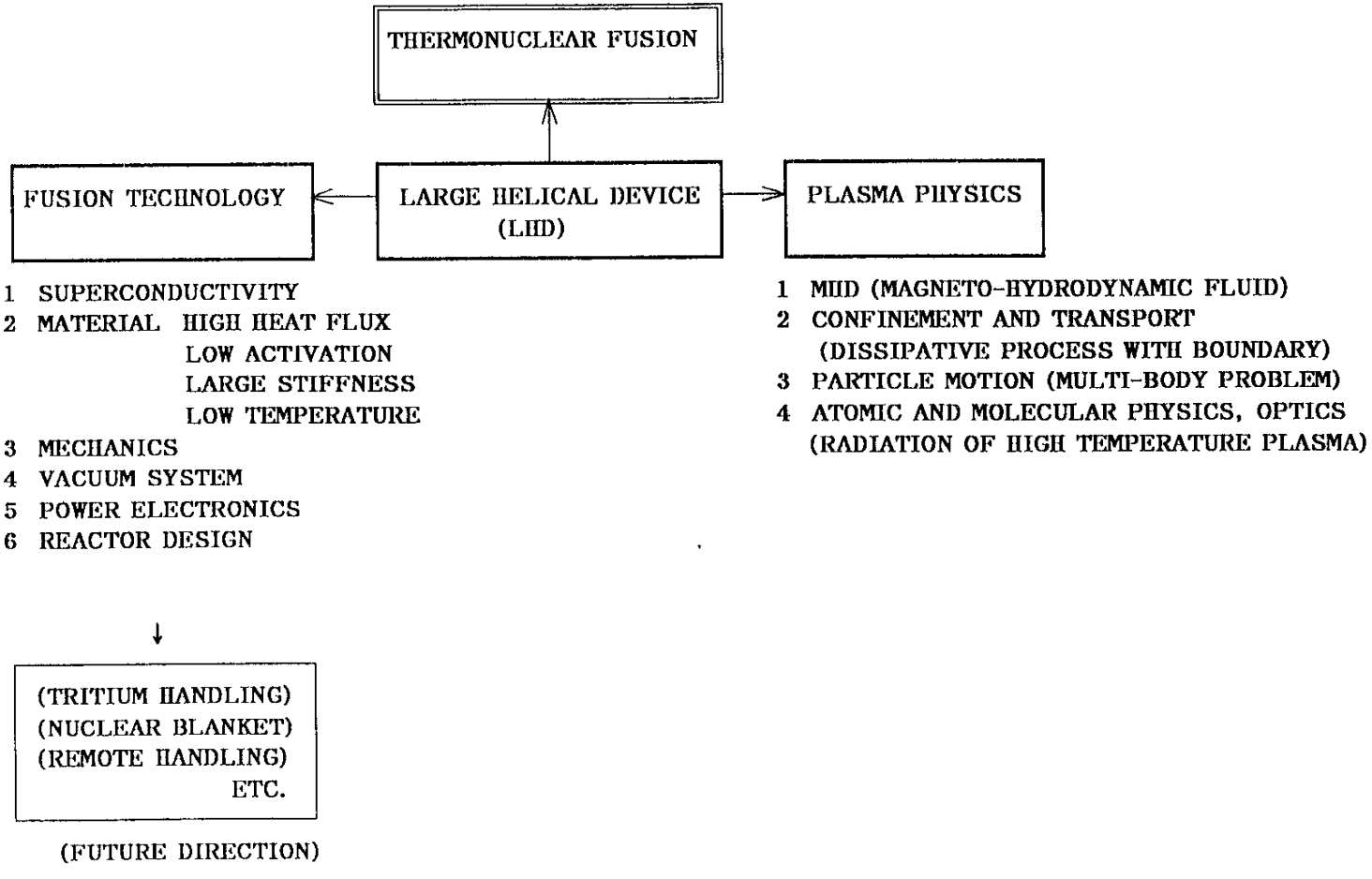
THERMONUCLEAR FUSION
FUSION TECHNOLOGY
LARGE HELICAL DEVICE
(LHD)
PLASMA PHYSICS
1 SUPERCONDUCTIVITY
2 MATERIAL HIGH HEAT FLUX
LOW ACTIVATION
LARGE STIFFNESS
LOW TEMPERATURE
3 MECHANICS
4 VACUUM SYSTEM
5 POWER ELECTRONICS
6 REACTOR DESIGN
1 MHD (MAGNETO-HYDRODYNAMIC FLUID)
2 CONFINEMENT AND TRANSPORT
(DISSIPATIVE PROCESS WITH BOUNDARY)
3 PARTICLE MOTION (MULTI-BODY PROBLEM)
4 ATOMIC AND MOLECULAR PHYSICS, OPTICS
(RADIATION OF HIGH TEMPERATURE PLASMA)
(TRITIUM HANDLING)
(NUCLEAR BLANKET)
(REMOTE HANDLING)
ETC.
(FUTURE DIRECTION)

Fig. 9

Recent Issues of NIFS Series

NIFS-109 Y. Kondoh, *Thought Analysis on Relaxation and General Principle to Find Relaxed State;* Sep. 1991

NIFS-110 H. Yamada, K. Ida, H. Iguchi, K. Hanatani, S. Morita, O. Kaneko, H. C. Howe, S. P. Hirshman, D. K. Lee, H. Arimoto, M. Hosokawa, H. Idei, S. Kubo, K. Matsuoka, K. Nishimura, S. Okamura, Y. Takeiri, Y. Takita and C. Takahashi, *Shafranov Shift in Low-Aspect-Ratio Heliotron / Torsatron CHS* ; Sep 1991

NIFS-111 R. Horiuchi, M. Uchida and T. Sato, *Simulation Study of Stepwise Relaxation in a Spheromak Plasma ;* Oct. 1991

NIFS-112 M. Sasao, Y. Okabe, A. Fujisawa, H. Iguchi, J. Fujita, H. Yamaoka and M. Wada, *Development of Negative Heavy Ion Sources for Plasma Potential Measurement* ; Oct. 1991

NIFS-113 S. Kawata and H. Nakashima, *Tritium Content of a DT Pellet in Inertial Confinement Fusion* ; Oct. 1991

NIFS-114 M. Okamoto, N. Nakajima and H. Sugama, *Plasma Parameter Estimations for the Large Helical Device Based on the Gyro-Reduced Bohm Scaling* ; Oct. 1991

NIFS-115 Y. Okabe, *Study of Au^- Production in a Plasma-Sputter Type Negative Ion Source* ; Oct. 1991

NIFS-116 M. Sakamoto, K. N. Sato, Y. Ogawa, K. Kawahata, S. Hirokura, S. Okajima, K. Adati, Y. Hamada, S. Hidekuma, K. Ida, Y. Kawasumi, M. Kojima, K. Masai, S. Morita, H. Takahashi, Y. Taniguchi, K. Toi and T. Tsuzuki, *Fast Cooling Phenomena with Ice Pellet Injection in the JIPP T-IIU Tokamak;* Oct. 1991

NIFS-117 K. Itoh, H. Sanuki and S. -I. Itoh, *Fast Ion Loss and Radial Electric Field in Wendelstein VII-Λ Stellarator*; Oct. 1991

NIFS-118 Y. Kondoh and Y. Hosaka, *Kernel Optimum Nearly-analytical Discretization (KOND) Method Applied to Parabolic Equations <<KOND-P Scheme>>;* Nov. 1991

NIFS-119 T. Yabe and T. Ishikawa, *Two- and Three-Dimensional Simulation Code for Radiation-Hydrodynamics in ICF*; Nov. 1991

NIFS-120 S. Kawata, M. Shiromoto and T. Teramoto, *Density-Carrying Particle Method for Fluid* ; Nov. 1991

NIFS-121 T. Ishikawa, P. Y. Wang, K. Wakui and T. Yabe, *A Method for the High-speed Generation of Random Numbers with Arbitrary Distributions;* Nov. 1991

NIFS-122 K. Yamazaki, H. Kaneko, Y. Taniguchi, O. Motojima and LHD Design Group, *Status of LHD Control System Design ; Dec. 1991*

NIFS-123 Y. Kondoh, *Relaxed State of Energy in Incompressible Fluid and Incompressible MHD Fluid* ; Dec. 1991

NIFS-124 K. Ida, S. Hidekuma, M. Kojima, Y. Miura, S. Tsuji, K. Hoshino, M. Mori, N. Suzuki, T. Yamauchi and JFT-2M Group, *Edge Poloidal Rotation Profiles of H-Mode Plasmas in the JFT-2M Tokamak ;* Dec. 1991

NIFS-125 H. Sugama and M. Wakatani, *Statistical Analysis of Anomalous Transport in Resistive Interchange Turbulence* ;Dec. 1991

NIFS-126 K. Narihara, *A Steady State Tokamak Operation by Use of Magnetic Monopoles* ; Dec. 1991

NIFS-127 K. Itoh, S. -I. Itoh and A. Fukuyama, *Energy Transport in the Steady State Plasma Sustained by DC Helicity Current Drive* ;Jan. 1992

NIFS-128 Y. Hamada, Y. Kawasumi, K. Masai, H. Iguchi, A. Fujisawa, JIPP T-IIU Group and Y. Abe, *New Hight Voltage Parallel Plate Analyzer* ; Jan. 1992

NIFS-129 K. Ida and T. Kato, *Line-Emission Cross Sections for the Charge-exchange Reaction between Fully Stripped Carbon and Atomic Hydrogen in Tokamak Plasma;* Jan. 1992

NIFS-130 T. Hayashi, A. Takei and T. Sato, *Magnetic Surface Breaking in 3D MHD Equilibria of l=2 Heliotron* ; Jan. 1992

NIFS-131 K. Itoh, K. Ichiguchi and S. -I. Itoh, *Beta Limit of Resistive Plasma in Torsatron/Heliotron* ; Feb. 1992

NIFS-132 K. Sato and F. Miyawaki, *Formation of Presheath and Current-Free Double Layer in a Two-Electron-Temperature Plasma* ; Feb. 1992

NIFS-133 T. Maruyama and S. Kawata, *Superposed-Laser Electron Acceleration* Feb. 1992

NIFS-134 Y. Miura, F. Okano, N. Suzuki, M. Mori, K. Hoshino, H. Maeda, T. Takizuka, JFT-2M Group, S.-I. Itoh and K. Itoh, *Rapid Change of Hydrogen Neutral Energy Distribution at L/H-Transition in JFT-*

2M H-mode ; Feb. 1992

NIFS-135 H. Ji, H. Toyama, A. Fujisawa, S. Shinohara and K. Miyamoto *Fluctuation and Edge Current Sustainment in a Reversed-Field-Pinch;* Feb. 1992

NIFS-136 K. Sato and F. Miyawaki, *Heat Flow of a Two-Electron-Temperature Plasma through the Sheath in the Presence of Electron Emission;* Mar. 1992

NIFS-137 T. Hayashi, U. Schwenn and E. Strumberger, *Field Line Diversion Properties of Finite β Helias Equilibria;* Mar. 1992

NIFS-138 T. Yamagishi, *Kinetic Approach to Long Wave Length Modes in Rotating Plasmas*; Mar. 1992

NIFS-139 K. Watanabe, N. Nakajima, M. Okamoto, Y. Nakamura and M. Wakatani, *Three-dimensional MHD Equilibrium in the Presence of Bootstrap Current for Large Helical Device (LHD)*; Mar. 1992

NIFS-140 K. Itoh, S. -I. Itoh and A. Fukuyama, *Theory of Anomalous Transport in Toroidal Helical Plasmas;* Mar. 1992

NIFS-141 Y. Kondoh, *Internal Structures of Self-Organized Relaxed States and Self-Similar Decay Phase;* Mar. 1992

NIFS-142 U. Furukane, K. Sato, K. Takiyama and T. Oda, *Recombining Processes in a Cooling Plasma by Mixing of Initially Heated Gas*; Mar. 1992

NIFS-143 Y. Hamada, K. Masai, Y. Kawasumi, H. Iguchi, A. Fijisawa and JIPP T-IIU Group, *New Method of Error Elimination in Potential Profile Measurement of Tokamak Plasmas by High Voltage Heavy Ion Beam Probes;* Apr. 1992

NIFS-144 N. Ohyabu, N. Noda, Hantao Ji, H. Akao, K. Akaishi, T. Ono, H. Kaneko, T. Kawamura, Y. Kubota, S. Morimoto. A. Sagara, T. Watanabe, K. Yamazaki and O. Motojima, *Helical Divertor in the Large Helical Device;* May 1992

NIFS-145 K. Ohkubo and K. Matsumoto, *Coupling to the Lower Hybrid Waves with the Multijunction Grill*; May 1992

NIFS-146 K. Itoh, S. -I.Itoh, A. Fukuyama, S. Tsuji and Allan J. Lichtenberg, *A Model of Major Disruption in Tokamaks*; May 1992

NIFS-147 S. Sasaki, S. Takamura, M. Ueda, H. Iguchi, J. Fujita and K. Kadota,

Edge Plasma Density Reconstruction for Fast Monoenergetic Lithium Beam Probing; May 1992

NIFS-148 N. Nakajima, C. Z. Cheng and M. Okamoto, *High-n Helicity-induced Shear Alfvén Eigenmodes*; May 1992

NIFS-149 A. Ando, Y. Takeiri, O. Kaneko, Y. Oka, M. Wada, and T. Kuroda, *Production of Negative Hydrogen Ions in a Large Multicusp Ion Source with Double-Magnetic Filter Configuration*; May 1992

NIFS-150 N. Nakajima and M. Okamoto, *Effects of Fast Ions and an External Inductive Electric Field on the Neoclassical Parallel Flow, Current, and Rotation in General Toroidal Systems*; May 1992

NIFS-151 Y. Takeiri, A. Ando, O. Kaneko, Y. Oka and T. Kuroda, *Negative Ion Extraction Characteristics of a Large Negative Ion Source with Double-Magnetic Filter Configuration*; May 1992

NIFS-152 T. Tanabe, N. Noda and H. Nakamura, *Review of High Z Materials for PSI Applications* ; Jun. 1992

NIFS-153 Sergey V. Bazdenkov and T. Sato, *On a Ballistic Method for Double Layer Regeneration in a Vlasov-Poisson Plasma*; Jun. 1992

NIFS-154 J. Todoroki, *On the Lagrangian of the Linearized MHD Equations*; Jun. 1992

NIFS-155 K. Sato, H. Katayama and F. Miyawaki, *Electrostatic Potential in a Collisionless Plasma Flow Along Open Magnetic Field Lines;* Jun. 1992

NIFS-156 O.J.W.F.Kardaun, J.W.P.F.Kardaun, S.-I. Itoh and K. Itoh, *Discriminant Analysis of Plasma Fusion Data*; Jun. 1992

NIFS-157 K. Itoh, S.-I. Itoh, A. Fukuyama and S. Tsuji, *Critical Issues and Experimental Examination on Sawtooth and Disruption Physics*; Jun. 1992

NIFS-158 K. Itoh and S.-I. Itoh, *Transition to H-Mode by Energetic Electrons*; July 1992

NIFS-159 K. Itoh, S.-I. Itoh and A. Fukuyama, *Steady State Tokamak Sustained by Bootstrap Current Without Seed Current*; July 1992

NIFS-160 H. Sanuki, K. Itoh and S.-I. Itoh, *Effects of Nonclassical Ion Losses on Radial Electric Field in CHS Torsatron/Heliotron*; July 1992